ELSEVIER

Biochimica et Biophysica Acta 1467 (2000) 153–164

BIOCHIMICA ET BIOPHYSICA ACTA
BBA

www.elsevier.com/locate/bba

Interactions of the HIV-1 fusion peptide with large unilamellar vesicles and monolayers. A cryo-TEM and spectroscopic study

Aitziber Agirre [a], Carol Flach [b], Félix M. Goñi [a], Richard Mendelsohn [b], José M. Valpuesta [c], Fangjun Wu [b], José L. Nieva [a,*]

[a] *Unidad de Biofísica (CSIC-EHU/UPV) y Departamento de Bioquímica, Universidad del País Vasco, Aptdo. 644, 48080 Bilbao, Spain*
[b] *Rutgers University, Department of Chemistry, Newark, NJ 07102, USA*
[c] *Centro Nacional de Biotecnología, CSIC, Universidad Autónoma de Madrid, 28049 Madrid, Spain*

Received 21 December 1999; received in revised form 28 March 2000; accepted 28 March 2000

Abstract

We have examined the interaction of the human immunodeficiency virustype 1 fusion peptide (23 amino acid residues) and of a Trp-containing analog with vesicles composed of dioleoylphosphatidylcholine, dioleoylphosphatidylethanolamine and cholesterol (molar ratio, 1:1:1). Both the native and the Trp-substituted peptides bound the vesicles to the same extent and induced intervesicular lipid mixing with comparable efficiency. Infrared reflection–absorption spectroscopy data are compatible with the adoption by the peptide of a main β-sheet structure in a cospread lipid/peptide monolayer. Cryo-transmission electron microscopy observations of peptide-treated vesicles reveal the existence of a peculiar morphology consisting of membrane tubular elongations protruding from single vesicles. Tryptophan fluorescence quenching by brominated phospholipids and by water-soluble acrylamide further indicated that the peptide penetrated into the acyl chain region closer to the interface rather than into the bilayer core. We conclude that the differential partition and shallow penetration of the fusion peptide into the outer monolayer of a surface-constrained bilayer may account for the detected morphological effects. Such single monolayer-restricted interaction and its structural consequences are compatible with specific predictions of current theories on viral fusion.

Keywords: Membrane fusion; Viral fusion; Human immunodeficiency virustype 1; Fusion peptide; Peptide–lipid interaction; Peptide conformation

1. Introduction

Viral and cellular membrane fusion events are mediated by specialized membrane proteins that help in overcoming the energetic barrier associated with the process [1,2]. Current models for the mech-

Abbreviations: Br_6-PSPC, 1-palmitoyl-2-stearoyl(6,7)dibromo-*sn*-glycero-3-phosphocholine; Br_{11}-PSPC, 1-palmitoyl-2-stearoyl(11,12)-dibromo-*sn*-glycero-3-phosphocholine; CHOL, cholesterol; cryo-TEM, cryo-transmission electron microscopy; DMSO, dimethyl sulfoxide; DOPC, dioleoylphosphatidylcholine; DOPE, dioleoylphosphatidylethanolamine; DOPG, dioleoylphosphatidylglycerol; DPPC-d_{62}, acyl chain-perdeuterated dipalmitoylphosphatidylcholine; DPPE, dipalmitoylphosphatidylethanolamine; HIV, human immunodeficiency virus; IRRAS, infrared reflection–absorption spectroscopy; LUV, large unilamellar vesicles; N-NBD-PE, *N*-(7-nitro-2,1,3-benzoxadiazol-4-yl) phosphatidylethanolamine; *N*-Rho-PE, *N*-(lissamine Rhodanine B sulfanyl) phosphatidylethanolamine

* Corresponding author. Fax: +34-94-4648500; E-mail: gbpniesj@lg.ehu.es

0005-2736/00/$ – see front matter
PII: S0005-2736(00)00214-5

anism of viral spike-mediated fusion involve the hydrophobic fusion peptide region that inserts into the target membrane [1,3]. In human immunodeficiency virustype 1 (HIV-1), the fusion peptide is located at the N-terminus of the gp41 transmembrane subunit of the envelope protein [4–7].

Several findings, including mutational analysis, support the direct involvement of this conserved segment of about 25 amino acids in HIV-1 fusion in vivo [5–7]. One important and unsolved issue is to establish whether the insertion of this sequence represents only a way to initially anchor the spike complex to the target membrane or if, in addition, the interaction of the peptides induces some kind of bilayer perturbation necessary for merging the viral and cell membranes [3,8]. Pioneering in vitro studies by Rafalski et al. [9] demonstrated the capacity of this sequence to bind and destabilize negatively charged model membranes composed of 1-palmitoyl-2-oleoyl-*sn*-glycero-3-phosphoglycerol. Since then several groups have published results that confirm and extend those observations [10–14].

The initial interaction and final conformation adopted by the HIV-1 fusion peptide in membrane bilayers appears to be governed by a plethora of experimental factors. Thus, synthetic sequences representing different sections of the gp41 N-terminus have been shown to interact with model membranes while adopting different conformations. Sequences representing the first 13 and 16 amino acids at gp41 N-terminus are mainly α-helical at low doses in neutral vesicles [15]. For even longer (23-residue) sequences, a predominant α-helical conformation has been shown in negatively charged vesicles and micelles [9,13,16] and in erythrocyte membranes at low doses [11]. However, under conditions allowing membrane fusion in vesicular systems (e.g. anionic and neutral vesicles containing increasing peptide loads) the 23-residue peptides adopt predominant β-type conformations [11,13,17–19]. For even longer (33-mer) versions of the peptide, mainly β-type conformations have been detected in bilayers composed of anionic phospholipids [20,21]. More recently, Schwarz and Taylor [22] have reported monolayer results also consistent with the existence of different structures in 23-residue peptides depending on the peptide load and monolayer compression.

Nieva et al. [17] and Pereira et al. [18] showed that a sequence of 23 amino acid residues at the N-terminus of HIV-1 gp41 has the capacity to destabilize large unilamellar vesicles made of an equimolar mixture of dioleoylphosphatidylcholine (DOPC), dioleoylphosphatidylethanolamine (DOPE) and cholesterol (CHOL). In contact with these membranes the peptide adopts a predominantly extended conformation. No alternative conformations are detected in this system by varying the peptide dose [18]. Kinetic analysis further suggests that the peptide acts as an agent that confers instability to membranes so that fusion can occur [13,17]. This implies that the β-structure or a precursor leading to its formation must be able to alter the local properties of the membrane in order to produce the detected perturbations. More recently, we have demonstrated by means of cryo-transmission electron microscopy (cryo-TEM) of diluted vesicles the formation of non-lamellar lipidic aggregates during the time course of lipid mixing induced by the peptide [23]. The cryo-TEM technique had previously been used for monitoring structural changes in liposomes supporting fusion [24–28] and was also quite successful in detecting the morphology changes experienced by vesicles interacting with the HIV-1 fusion peptide.

In the present study we attempt to elucidate the molecular mechanism underlying the membrane activity of the HIV-1 fusion peptide under conditions inducing the adoption of a predominantly β-type conformation. The structure of the peptide in lipid monolayers at the air–water interface has been evaluated over a wide range of lateral pressures by infrared reflection–absorption spectroscopy (IRRAS). In addition, we have made use of the invaginated morphology present in DOPC:DOPE:CHOL extruded vesicles in order to infer the location of the peptide initially partitioning into the membrane. Loss of invagination in extruded large unilamellar vesicles (LUV) has been previously used to test changes in internal vesicle volume and monolayer areas [29,30]. In this study, we have focused our attention on the fraction of the peptide-treated vesicles remaining isolated or at the periphery of large lipidic aggregates. Consistent with a preferential increase of the external monolayer surface under isotonic conditions, the invagination disappears in peptide-treated vesicles. Trp fluorescence was subsequently used to probe the depth of peptide insertion into the membrane. For

this purpose the phenylalanine in position 8 was substituted by a tryptophan residue, the resulting peptide F8W being equally active as the original one in vesicle destabilization and fusion. The peptide was shown to insert close to the interface and promoted the formation of protrusions in the surface-restricted bilayer of isolated vesicles. These findings are discussed in relation to a putative role of fusion peptides within the spike complex that mediates the viral fusion event.

2. Materials and methods

DOPC, DOPE, dipalmitoylphosphatidylcholine (DPPC), acyl chain-perdeuterated dipalmitoylphosphatidylcholine (DPPC-d_{62}), dipalmitoylphosphatidylethanolamine (DPPE) and the brominated phospholipids 1-palmitoyl-2-stearoyl(6,7)dibromo-*sn*-glycero-3-phosphocholine (Br_6-PSPC) and 1-palmitoyl-2-stearoyl(11,12)dibromo-*sn*-glycero-3-phosphocholine (Br_{11}-PSPC) were purchased from Avanti Polar Lipids (Birmingham, AL, USA). CHOL was obtained from Sigma (St. Louis, MO, USA). All other reagents were of analytical grade. The sequences representing the 23 amino acids at the N-terminus of the HIV-1 gp41 [18] were synthesized as their C-terminal carboxamide and purified (estimated homogeneity $>90\%$) by Quality Controlled Biochemicals, Inc. (Hopkinton, MA, USA). Peptide stock solutions were prepared in dimethyl sulfoxide (DMSO, spectroscopy grade).

LUV consisting of DOPC, DOPE and CHOL (molar ratio, 1:1:1) were prepared according to the extrusion method of Hope et al. [31] in 5 mM HEPES, 100 mM NaCl (pH 7.4). Lipid concentrations of liposome suspensions were determined by phosphate analysis [32]. The mean diameter of DOPC/DOPE/CHOL vesicles was 130 nm as estimated by quasielastic light scattering using a Malvern Zeta-Sizer instrument.

Membrane lipid mixing was monitored using the resonance energy transfer assay, described by Struck et al. [33]. The assay is based on the dilution of the fluorescent probes N-(7-nitrobez-2-oxa-1,3-diazol-4-yl) phosphatidylethanolamine (N-NBD-PE) and N-(lissamine Rhodamine B sulfonyl) phosphatidylethanolamine (N-Rho-PE). Dilution due to membrane mixing results in an increase in *N*-NBD-PE fluorescence. Vesicles containing 0.6 mol% of each probe were mixed with unlabeled vesicles at a 1:4 ratio. The NBD emission was monitored at 530 nm with the excitation wavelength set at 465 nm. A cutoff filter at 515 nm was used between the sample and the emission monochromator to avoid scattering interferences. The fluorescence scale was calibrated such that the zero level corresponded to the initial residual fluorescence of the labeled vesicles and the 100% value to complete mixing of all the lipids in the system. The latter value was set by the fluorescence intensity of vesicles, labeled with 0.12 mol% each of the fluorophores, at the same total lipid concentration as in the fusion assay.

The amount of membrane-bound peptide was estimated by monitoring the fluorescence of the Trp residue in the F8W analog. By following a previously published procedure [18,34], unbound peptide was separated from bound peptide by ultracentrifugation in D_2O buffer. Floated membranes containing bound peptide were solubilized with 2 mM octaethyleneglycol monododecyl ether ($C_{12}E_8$) to minimize the scattering contribution of membranes to Trp fluorescence. The Trp signal at 333 nm was normalized for the amount of co-floating lipid which was simultaneously quantified also by means of spectrofluorimetry. To that end, we used the same liposomes as for the lipid mixing assay containing a fraction (20%) labeled with 0.6 mol% of *N*-NBD-PE and *N*-Rho-PE. In addition to lipid quantification, NBD and Rho fluorescence measurements provided verification of complete vesicle solubilization by $C_{12}E_8$.

The samples for cryo-TEM were prepared following two different protocols. In one protocol the peptide and the liposomes were mixed under continuous stirring at 37°C. At defined post-mixing times, drop samples were collected from the mixtures and applied to holey carbon films, quickly blotted and frozen in liquid ethane at −180°C, so that the vesicles were preserved in vitreous ice. Alternatively, liposome–peptide mixtures prepared in D_2O buffer were floated as described before. In brief, the mixtures were incubated for 30 min at 37°C, then overnight at room temperature and subsequently subjected to ultracentrifugation ($600\,000\times g$) for 2 h in D_2O buffer. Samples collected from the top (floating fraction) were subsequently applied to the holey carbon films as

in the previous case. The frozen grids were kept under liquid nitrogen until used. Electron micrographs were obtained using a Jeol 1200EX II operated at 120 kV and equipped with a GATAN-626 cold stage and a GATAN anticontaminator. Images were obtained with a nominal magnification of $\times 50\,000$ and an underfocus of 15 000–20 000 Å, and recorded on Kodak SO-163 film developed at full strength for 12 min in D-19 developer.

For IRRAS monolayer experiments an equimolar solution of DPPC-d_{62}/DPPE/CHOL was prepared in chloroform:methanol (4:1, v:v) at a total concentration of $\sim$2 mg/ml. Phospholipids with saturated acyl chains were chosen for monolayer studies due to their greater film stability when compared to their unsaturated counterparts. A 1 mg/ml peptide solution was prepared in DMSO. Appropriate amounts of each solution were mixed to yield a total lipid to peptide molar ratio of 14:1. A subphase of 5 mM Tris, 100 mM NaCl, 2 μM EDTA was prepared in D_2O, pD $\approx$ 7.4. A D_2O-based subphase was used for the IRRAS measurements to avoid interference from the H_2O bending mode at 1640 cm^{-1} and to lessen the effects of the rotational–vibrational modes of H_2O vapor in the same spectral region. Details of the IRRAS trough and optical set-up have been described elsewhere [35]. The temperature of the subphase was held at 21.5 ± 0.5°C. Spreading volumes ranged from $\sim$8.0 μl for the cospread lipid/peptide films to $\sim$14.0 μl for the pure peptide films. This resulted in initial surface pressure values of 0 mN/m at a maximum surface area of $\sim$89 cm^2. After an initial relaxation period of 1 h, films were intermittently compressed over a 3–4 h period until the desired surface pressure was reached. IRRAS spectra were acquired using a Bio-Rad FTS 40A spectrometer (Cambridge, MA, USA) equipped with an MCT detector. The experiments were conducted at a 35° angle of incidence (angle between the incoming beam and surface normal). A shuttle device was employed to compensate for atmospheric water vapor. Typically eight blocks of 128 scans each were acquired at 4 cm^{-1} resolution, co-added, apodized with a triangular function, and Fourier-transformed with one level of zero-filling to yield spectra encoded at 2 cm^{-1} intervals. IRRAS spectra are presented as reflectance–absorbance (RA) versus wavenumber. RA is defined as $-\log(R/R_0)$, where R is the reflectivity of the film-covered surface and R_0 is the reflectivity of the film-free surface. When necessary residual water vapor was subtracted from spectra. Peak positions were determined using a center of gravity algorithm written at the National Research Council of Canada.

The depth of peptide penetration into the membrane was evaluated using the analog of the fusion peptide containing the F8W substitution. Quenching of Trp fluorescence by the hydrophobic matrix-residing bromolipids was assayed as described by Bolen and Holloway [36]. Quenching by the water-soluble acrylamide was carried out following the methodology described by De Kroon et al. [37] and Moro et al. [38]. In both assays, lipid–peptide mixtures (1 μM peptide, 100 μM lipid) were incubated at 37°C for 10 min and then at room temperature for 1 h before data acquisition. In the case of the bromolipid assay, either Br_6-PSPC or Br_{11}-PSPC was used instead of DOPC in target vesicles. Corrected Trp emission spectra were acquired in a Perkin-Elmer MPF-66 spectrofluorimeter. Five spectra were currently averaged from each sample. In the acrylamide experiments Trp emission was recorded at the fixed wavelength of 345 nm. Excitation was set at 295 nm in order to reduce acrylamide absorbance. Emitted fluorescence at increasing concentrations of acrylamide was corrected for dilution, scatter contributions and absorptive screening by acrylamide [37]. Data were analyzed according to the Stern–Volmer equation for collisional quenching:

$$F_0/F = 1 + K_{sv}[Q]$$

where F_0 and F are the fluorescence intensities in the absence and presence of the quencher, Q, and K_{sv} is the Stern–Volmer quenching constant. In the range of acrylamide concentrations used (1–60 mM) the Stern–Volmer plots did not deviate from linearity.

3. Results

3.1. Peptide-induced intervesicular lipid mixing

The activity of the parental HIV-1 fusion peptide was comparatively studied together with the F8W substitution-containing analog in terms of their ability to bind lipid bilayers and induce lipid mixing. This was intended to establish a quantitative rela-

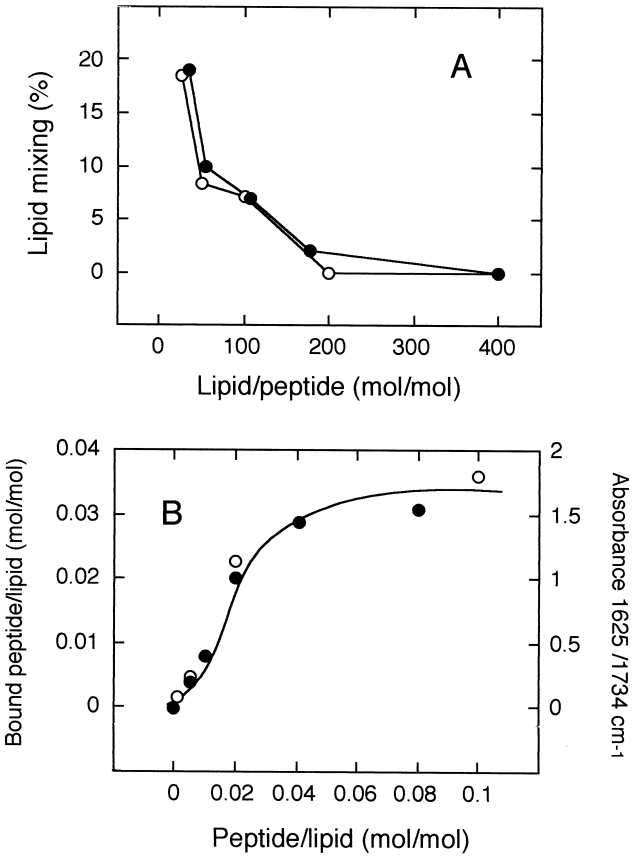

Fig. 1. (A) Extent of membrane lipid mixing of DOPC/DOPE/CHOL (1:1:1) LUV induced by the HIV-1 fusion peptide (open circles) and its F8W analog (filled circles) as a function of lipid-to-peptide molar ratio. Vesicle concentration was 100 μM. (B) Saturation curves of the amount of peptide bound per lipid in floated DOPC/DOPE/CHOL (1:1:1) LUV as a function of the added peptide-to-lipid ratio. The peptide was added to LUV (1 mM) at different peptide-to-lipid ratios, incubated for 30 min at 37°C and then overnight at room temperature. The formed peptide–lipid complexes were subsequently isolated from the floating fractions after ultracentrifugation in D_2O buffer. Filled circles: amount of F8W analog bound per lipid as estimated from Trp fluorescence associated with the floating vesicles; open circles: $I_{1625\ cm^{-1}}/I_{1734\ cm^{-1}}$ ratio as estimated from FTIR data of HIV-1 fusion peptide associated with vesicles [18].

tionship between the morphological changes detected in peptide-treated DOPC/DOPE/CHOL vesicles and the peptide dose required in the membrane to induce such alterations. As shown in Fig. 1A, the fluorescent peptide analog containing the F8W substitution was as effective as the parental HIV-1 sequence in promoting lipid mixing over a wide range of peptide concentrations. This observation confirms the functional equivalence of both sequences.

The use of a fluorescent analog allows, among other things, an estimation of the amount of membrane-bound peptide by monitoring the fluorescence of the Trp residue (see Section 2). In Fig. 1B the amount of bound peptide per lipid, as estimated from Trp fluorescence, is plotted together with the binding data deduced from Fourier transform infrared (FTIR) measurements performed on floated DOPC/DOPE/CHOL vesicles that had been treated with variable doses of the parental peptide [18]. In those samples, the ratio of the amide I absorbance at 1625 cm^{-1} (absorption of the extended structure of the peptide) to that at 1734 cm^{-1} arising from the C=O stretching vibration of the phospholipid ester bonds is proportional to the peptide-to-lipid ratio in the membrane. As shown in Fig. 1B, both sets of data can be fitted to a single curve that shows saturation at values corresponding roughly to 35 lipids per bound peptide.

3.2. Peptide conformation in a lipidic environment

The IRRAS spectrum of the lipid carbonyl and amide I region for a cospread lipid (DPPC-d_{62}/DPPE/CHOL)/peptide monolayer on D_2O buffer is shown in Fig. 2. The presence of the amide I vibra-

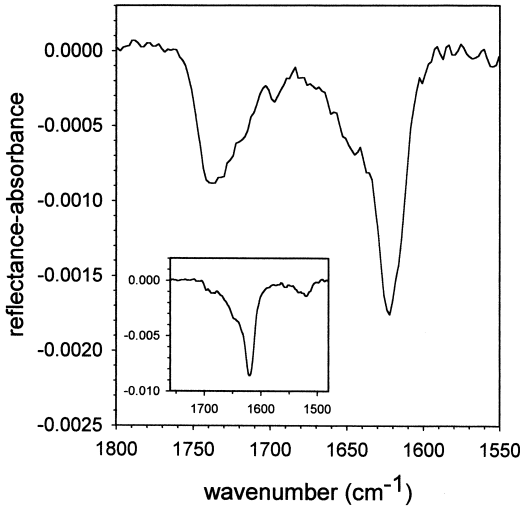

Fig. 2. IRRAS spectrum of (DPPC-d_{62}/DPPE/CHOL)/peptide monolayer (total lipid-to-peptide molar ratio, 14:1) on D_2O buffer at a surface pressure of 8 mN/m. The inset displays IRRAS spectrum of pure peptide monolayer under the same conditions.

tional mode at 1623 cm^{-1} is indicative of deuterium-exchanged β-sheet secondary structure. Minor contributions to the amide I band contour in the 1640–1660 cm^{-1} region may result from random coil or helical structure. The absence of an amide II band, in the 1550 cm^{-1} region (not shown), signifies that the hydrogen–deuterium exchange is essentially complete. The lipid carbonyl band is observed at ~1735 cm^{-1}.

The inset in Fig. 2 displays the IRRAS spectrum of a pure peptide monolayer. The predominant amide I band is observed at 1620 cm^{-1}, with a shoulder in the 1640–1650 cm^{-1} region, and a less intense component at ~1690 cm^{-1}. The presence of both high and low frequency components (1690, 1620 cm^{-1}) and their relative intensities indicate that the peptide forms antiparallel β-sheet structures at the air–D_2O interface. The less intense component may be just discernible in the binary monolayer spectrum at ~1690 cm^{-1}, however, the low signal to noise level makes it difficult to assign this band with certainty. The lower frequency observed for the main amide I peak of the pure peptide monolayer compared to the binary system suggests a slightly more extended or aggregated β-sheet-type structure for the former [39]. In the inset, residual amide II band intensity is observed between 1500 and 1550 cm^{-1} indicating that a small number of peptide groups have not been deuterium-exchanged. These findings would be consistent with the existence of an interaction between lipid and peptide in the binary system. Moreover, they indicate that, most likely as a consequence of such an interaction, pure peptide differs structurally from the peptide associated with the lipid monolayer.

Additional evidence that the spectrum in Fig. 2 is characteristic of peptides interacting with hosting lipids comes from the fact that the amide I band position for this lipid/peptide monolayer does not change over a pressure range from 6 to 27 mN/m (data not shown). If the peptide existed on the surface in lipid-free separated domains, we would expect a lower amide I frequency (similar to the same position as the pure peptide). This also indicates that under those measuring conditions, altering the monolayer lateral pressure did not induce any appreciable conformational change. Pereira et al. [18] found for DOPC:DOPE:CHOL LUV that the structure adopted by the peptide at equilibrium was mainly an extended one at peptide-to-lipid molar ratios ranging from 1:800 to 1:10. Both findings suggest that this lipid matrix containing the peptide represents a homogeneous system in the sense that the peptide conformation is locked into one single structure under a variety of membrane conditions. Consistency of secondary structure in the bilayer versus monolayer environments is not necessarily anticipated as peptides and proteins have been previously shown to have different conformations in these two different systems [40].

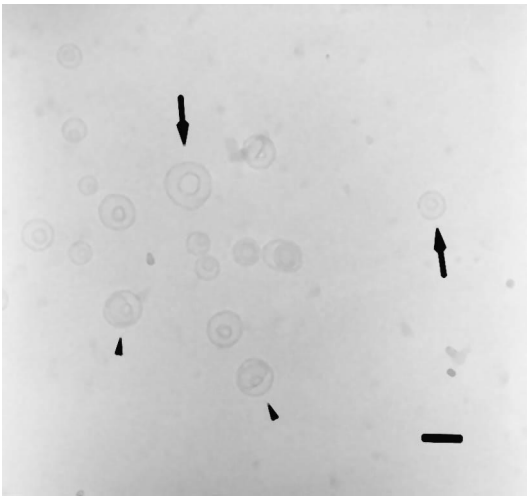

Fig. 3. Cryo-TEM micrograph of control extruded LUV of DOPC/DOPE/CHOL (1:1:1) showing stomatocyte-like morphology. Arrowheads: vesicles oriented showing the open neck. Arrows: vesicles oriented such that the symmetry axis is perpendicular to the projection plane. Bar: 100 nm.

3.3. *Effect on vesicle morphology*

Cryo-TEM micrographs of vitrified DOPC/DOPE/CHOL unilamellar vesicles obtained from floating fractions (Fig. 3) showed a majority of vesicles (approx. 90%) whose stomatocyte-like morphology suggested the existence of an initial invaginated state. The remaining vesicle population (approx. 10%) consisted of spherical vesicles and, therefore, the presence of morphologies others than spherical or invaginated in our DOPC/DOPE/CHOL unilamellar vesicles obtained through extrusion [31] can be excluded. This observation is critical to infer the localization of the membrane-partitioning peptide through the loss of the initial invagination state

(see below). A detailed view of a representative example of such predominantly invaginated non-spherical vesicles is shown in Fig. 4a. The picture, obtained from a sample vitrified at 37°C, illustrates the invaginated morphology in which the rounded open neck connecting the internal and external vesicles can be easily discerned (arrowhead).

It is well established that the extrusion process used to generate LUV renders non-spherical systems [24,29]. As discussed by Mui et al. [30], the shear tensions during the process may generate differences between internal and external monolayer areas, whose range may be specific for the lipid composition and other experimental conditions used during the extrusion procedure. The DOPC/DOPE/CHOL (1:1:1) LUV samples that we obtained through extrusion (Fig. 3) structurally resemble the DOPC/dioleoylphosphatidylglycerol (DOPG) (9:1) and DOPC/DOPG/CHOL (6:1:3) LUV samples obtained by Mui et al. [30] in that they mainly consist of stomatocytes. These authors showed that such an initial condition could be used to test in LUV the morphological consequences of generating a transbilayer area asymmetry. They demonstrated that increasing the external monolayer surface area by inducing transbilayer transport of phospholipids eventually transforms invaginated LUV into beaded-tubular structures or spherical structures with one or more membrane protrusions.

Starting from an analogous invaginated LUV sample, we have studied here the morphological effect of HIV-1 peptide addition. Following the reasoning of Mui et al. [30], we expected to infer from changes in the morphology of our invaginated LUV whether the peptide did or did not preferentially partition into the external monolayer increasing its surface. If the peptide instantaneously redistributed among both monolayers and/or adopted a transmembrane orientation it would not differentially affect monolayer surfaces, and morphology changes would not be expected. As shown in Fig. 4b–e a morphology consist-

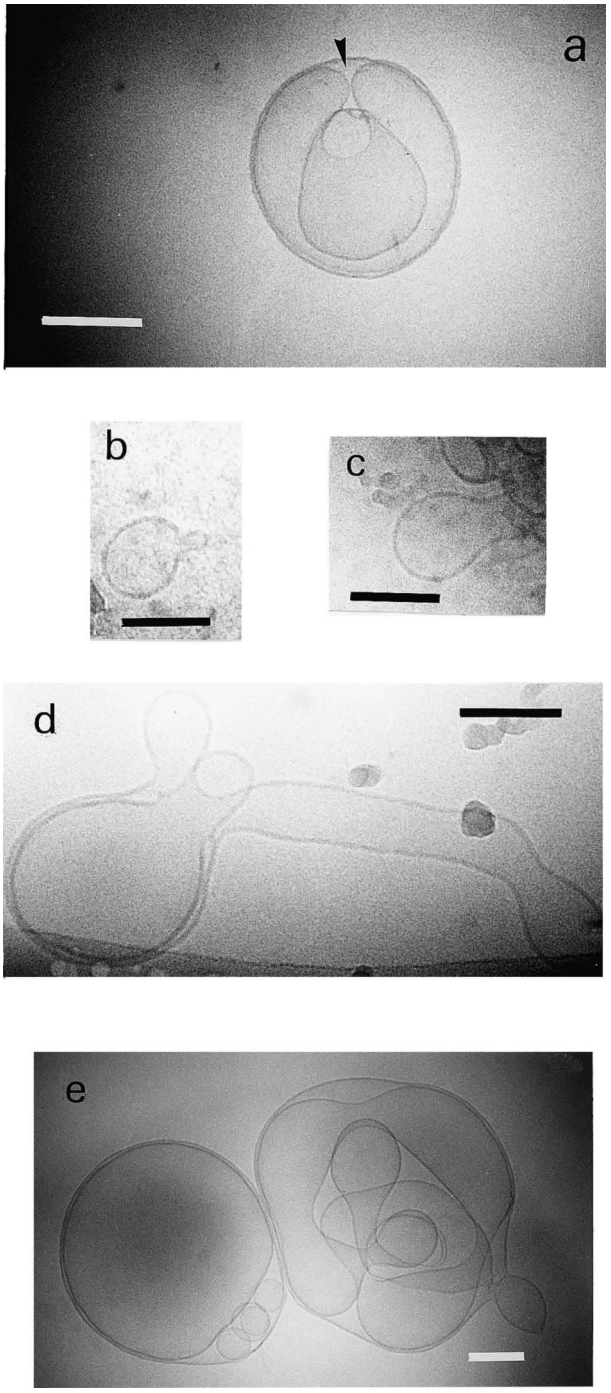

→

Fig. 4. Cryo-TEM micrographs of LUV of DOPC/DOPE/CHOL (1:1:1) vitrified at various times after peptide addition (peptide-to-lipid molar ratio 1:10, i.e. saturating conditions) showing membrane protrusions. (a) Detailed view of a LUV of DOPC/DOPE/CHOL (1:1:1) before peptide addition (time = 0) showing invaginative processes, the arrowhead indicates the open rounded neck. (b, c) Time = 9 s. (d) Time = 55 s. (e) Peptide-treated vesicles after flotation in D_2O buffer, in this case vesicles (1 mM) were mixed with the peptide as before at 37°C, incubated for 30 min and then overnight at room temperature before ultracentrifugation in D_2O buffer (2 h at 600 000 × *g*). Bars: 100 nm. These micrographs are representative examples of nine processed samples and 47 different grid areas explored.

ing of membrane protrusions and beaded tubes could be observed in HIV-1 fusion peptide-treated vesicles. In fact only 30% of the non-aggregated vesicles remained invaginated in those samples. Morphological changes reflected in Fig. 4b–e compared to Fig. 4a are consistent with the induction by the peptide of a preferential increase of the external monolayer area, with little or no change in vesicle volume [30].

It must be pointed out that these micrographs correspond to grid regions where single vesicles could be discerned either isolated or at the edge of large aggregates that were also formed as a consequence of the peptide interaction [23]. Those aggregates show a characteristic compact morphology consisting of highly bent lamellae and multiple attachments, and represent probably a non-lamellar organization of the peptide–lipid complexes. Formation of those structures must involve multiple fusion events making it possible that membranes of different sidedness become contiguous, a process that by itself could relieve transbilayer stress. We must thus caution that the morphology of large fused vesicles incubated for long times, such as those shown in Fig. 4e, could have originated from multiple fusion events.

The IRRAS spectrum depicted in Fig. 2 for the peptide and a lipid monolayer was acquired at a peptide-to-lipid molar ratio of 1:14, equivalent to a 1:28 molar ratio in a bilayer system in which only one monolayer contained the peptide. Under the conditions used to evaluate morphology changes in Fig. 4 vesicles became saturated at about 1:35 (see Fig. 1). So the cryo-TEM and IRRAS experiments were conducted at comparable peptide-to-lipid molar ratios. This, together with the fact that the same secondary structure is observed for bilayers and monolayers, indicates that the peptide structure inferred from IRRAS experiments is likely to reflect the structure that the peptide interacting with vesicles eventually adopts in cryo-TEM samples.

Taken together, the IRRAS and cryo-TEM results suggest that in our system it is the initial differential partitioning of the peptide into the external monolayer of isolated vesicles that induces differences between the surface areas of the two monolayers. This phenomenon could be at the origin of the dramatic changes in vesicle morphology described. It should be noted that this peptide effect would only occur in surface-restricted systems such as the closed vesicles used in this study, where the difference in surface areas between the inner and outer monolayers cannot be balanced through the recruitment of lipids [29,30].

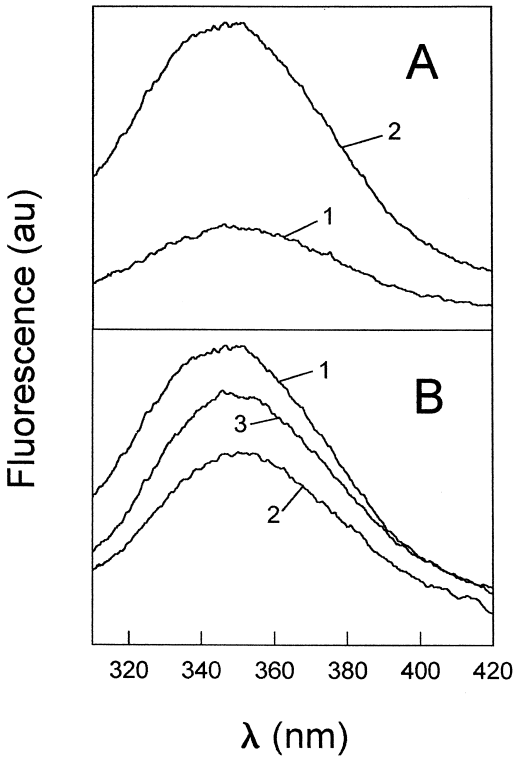

Fig. 5. (A) Fluorescence emission spectra of the F8W analog in buffer (1), and incubated with DOPC/DOPE/CHOL LUV (2). Vesicle concentration was 0.1 mM and the peptide-to-lipid ratio 1:100. (B) Fluorescence emission spectra of F8W analog incubated with LUV (0.1 mM) containing brominated phospholipids: (1) DOPC/DOPE/CHOL; (2) Br_6-PSPC/DOPE/CHOL; (3) Br_{11}-PSPC/DOPE/CHOL. Peptide-to-lipid ratio as in A. Lipid–peptide mixtures were incubated at 37°C for 10 min and then at room temperature for 1 h before data acquisition.

3.4. Depth of penetration

The peptide containing the F8W substitution was also used to estimate the depth of its penetration into the bilayer. Control experiments performed in the presence of this Trp analog demonstrated the ability of this sequence to promote a similar morphology to that induced by the parental peptide in DOPC/DOPE/CHOL vesicles (data not shown). Results displayed in Figs. 5 and 6 provide strong evidence that the fusion peptide penetrates into the membrane to the level of the acyl chains.

In Fig. 5A the emission spectra of the peptide in solution and in the presence of DOPC/DOPE/CHOL large unilamellar vesicles are compared. Trp emission intensity was significantly enhanced in the presence of the vesicles. This effect suggests that the Trp residue in the presence of vesicles was 'sensing' a less polar environment which is indicative of peptide penetration into the hydrophobic core of the bilayer. The bilayer level to which the peptide penetrated can be deduced from the spectra displayed in Fig. 5B Both Br_6-PSPC- and Br_{11}-PSPC-containing LUV quenched Trp fluorescence to some extent, but the former vesicles showed a higher quenching efficiency. Bromine atoms quench by a short-range process that requires a close approach to the fluorophore [36]. This would mean that the Trp residue must be located closer to the C_6-C_7 than to the C_{11}-C_{12} position within the acyl chain region of the bilayer.

Peptide penetration was further confirmed by the results obtained using the aqueous quencher acrylamide (Fig. 6). We selected this particular quencher since non-polar fluorophores embedded in the bilayer are not quenched by it [38]. For the peptide in buffer the Stern–Volmer quenching constant (K_{sv}) obtained from the plot depicted in the figure was 22.9 M^{-1}. In the presence of DOPC/DOPE/CHOL LUV, the obtained K_{sv} values were 21.4 M^{-1} for the water-soluble Trp analog *N*-acetyl-L-tryptophanamide and 9.8 M^{-1} for the HIV-1 fusion peptide. Since *N*-acetyl-L-tryptophanamide is fully accessible to acrylamide [41], those data indicate that the accessibility of the aqueous quencher to the Trp residue in the fusion peptide in the presence of vesicles was markedly reduced, a fact that is consistent with penetration of the peptide into the matrix of the bilayer.

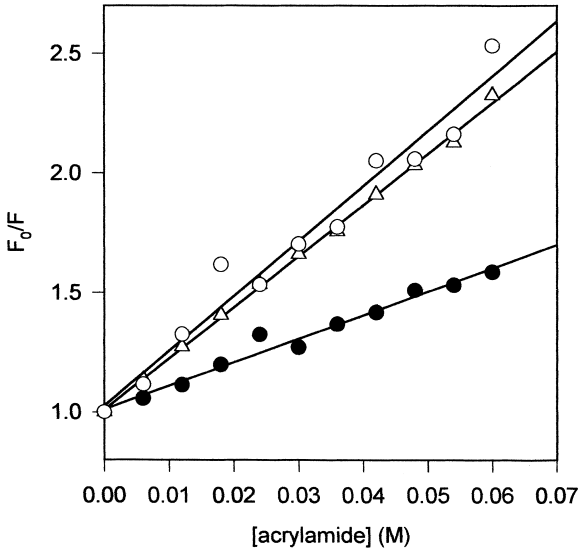

Fig. 6. Stern–Volmer plot of Trp fluorescence quenching of F8W analog by increasing concentrations of acrylamide, in solution (open circles) and in the presence of 100 μM DOPC/DOPE/CHOL LUV (filled circles) (peptide-to-lipid molar ratio, 1:100). A mixture of *N*-acetyl-L-tryptophanamide in the presence of liposomes (triangles) was used to obtain a reference curve corresponding to 100% solvent-exposed residues.

4. Discussion

4.1. Interaction of the HIV-1 fusion peptide with membranes

Taking into account the experimental results in this work, i.e. adoption by the peptide of an extended structure in lipid monolayers, induction of membrane protrusions in extruded vesicles, and penetration into the hydrophobic milieu of the bilayer, we can suggest a picture of how the HIV-1 fusion peptide interacts with DOPC/DOPE/CHOL membranes. Our suggestion is twofold.

First we propose that the interaction of the peptide adopting an extended structure is *restricted to the outer membrane monolayer*. The IRRAS data show that the peptide adopts the same β secondary structure in lipid monolayers as it does in vesicles [18]. In addition, the membrane protrusions in Fig. 4 would be consistent with a differential increase in the area of the vesicle external monolayer, caused by the preferential partition of the externally added peptide to surface-constrained bilayers (i.e. vesicle bilayers). In other words, loss of the initial invagination state is caused by the preferential insertion of the peptide in the external monolayer of the vesicle. To our knowledge this morphological transition induced in vesicles by a viral fusion peptide had not been previously described.

Second, we suggest that the peptide remains *close to the lipid–water interface* when inserted into the membrane. Assuming the bilayer and hydrocarbon chain region thicknesses to be 50 and 30 Å respectively, and the bromine distances from the bilayer

center 11 Å for 6,7 labels and 6.5 Å for 11,12 labels [42], the results in Figs. 5 and 6 would be consistent with a location of the Trp residue in the acyl chain region closer to the interface (~4 Å) than to the bilayer core (~11 Å). The shallow penetration of the peptide in one of the monolayers could induce the differential surface increase that is at the origin of the loss of the invaginated morphology of the vesicles.

Preferential insertion of a fusion peptide into the external monolayer has been previously demonstrated by Brunner [43] for the influenza fusion peptide. This author showed by means of hydrophobic photolabeling techniques that the fusion peptide at the N-terminus of bromelain-solubilized ectodomain of influenza hemagglutinin contacts only the outer leaflet of the liposome bilayer. More recently, using micropipette aspiration and video microscopy of large unilamellar vesicles, Longo et al. [44] have demonstrated that the interaction of a synthetic peptide representing the N-terminus of influenza hemagglutinin results in a large increase in membrane surface area. Incorporation of the peptide is subsequently followed by permeation through discrete pores and eventual rupture of the permeability barrier. Our results in this and previous works would be consistent with a similar behavior of the HIV-1 fusion peptide. The morphological data described here are compatible with membrane area expansion specifically exerted on the external monolayer. Leakage assays demonstrate that the peptide permeabilizes isolated vesicles [17,18] and the very existence of the aggregation and fusion processes taking place thereafter [23] seems to indicate that the peptide is able to perturb the lipid–water interface when it associates with membranes. Breaking down the continuity of monolayers may result in some exposure of the hydrophobic interior to the surrounding water which would in turn promote aggregation and fusion in vesicle suspensions. Membrane destabilization by peptides lying parallel to the membrane plane, and located in the outer monolayer in a 'carpet-like' fashion, has been proposed in several instances for widely different peptides and proteins [45–47].

4.2. Implications for the fusion mechanism

In a recent report on membrane fusion catalyzed by influenza hemagglutinin Chernomordik et al. [48] have proposed the involvement of a structural intermediate consisting of a ring of activated spikes that would restrict the flux of the enclosed lipids. Several indications suggest that HIV-1 gp41 activation is highly reminiscent of hemagglutinin activation [49,50]. If this is the case, it might be possible that one of the roles of the activated spike complex in promoting HIV-1 fusion would be to restrict lipid lateral diffusion in a defined area of the target membrane. If the HIV-1 fusion peptide is to insert into a bounded section of the target membrane, one may speculate on the consequences that such an interaction may have for the bilayer structure.

According to the experimental results described in this work, the local interaction of the HIV-1 gp41 N-terminal sequence with the target membrane might induce an increase in the external leaflet surface (*cis* contacting monolayer). Membrane stress might then be relaxed by two mechanisms operating simultaneously. The bilayer could change its shape giving rise to local and transient evaginations, and the internal monolayer (*trans* monolayer) might become stretched and locally thinned as the peptide was preferentially inserted into the external monolayer.

The hypothetical membrane destabilization described may reasonably be integrated within the body of the 'stalk mechanism' theory of fusion [51,52]. The stalk is a transient lipidic intermediate locally connecting the *cis* monolayers of apposed membranes. This intermediate is proposed to evolve towards hemifusion intermediates that eventually form the fusion pore, the final structure connecting both sides of the membranes in apposition and allowing mixing of aqueous contents. Stalk formation requires local destabilization of the contacting monolayers and exposure of hydrophobic groups. It has been argued that membrane adhesion might be facilitated at the peak of localized membrane protrusions [53]. Our experimental results indicate that the peptide insertion within a surface-constrained area might constitute a factor that would help in the formation of those protruding structures, and consequently also in the formation of the stalk.

According to the 'modified stalk' theory for fusion [28,52], the structural intermediates that follow stalk formation are *trans* monolayer contacts (TMCs), or local points of restricted hemifusion. Rupture of the

single bilayer diaphragm in TMCs would constitute the limiting step in the formation of the interlamellar attachments or fusion pores. These authors propose that viral fusion peptides could facilitate the formation of fusion pores by lowering the rupture tension of the TMC diaphragm. For instance, a putative mechanism, suggested by Siegel and Epand [28], might be a peptide-induced reduction of the lipid cohesion through a local change of bilayer thickness. Our experimental work suggests that, within surface-restricted bilayers, HIV-1 fusion peptide insertion into *cis* monolayers might result in concomitant thinning of *trans* monolayers, a process that would likely reduce their cohesion. So, a TMC bilayer diaphragm composed of stressed *trans* monolayers would probably be more prone to rupture and fusion pore formation would become easier/faster.

Acknowledgements

A.A. was the recipient of a predoctoral fellowship of the Basque Government. This work was supported by DGCYT (Grant PB96-0171), the Basque Government (PI 96-46; EX-1998-28; PI-1998-32) and the University of the Basque Country (UPV 042.310-EA085/97; UPV 042.310-G03/98). CICYT Grant BI097-0820-C02-01 (to J.M.V.) is also acknowledged.

References

[1] L.D. Hernández, L.R. Hoffman, T.G. Wolfsberg, J.M. White, Annu. Rev. Cell Dev. Biol. 12 (1996) 627–661.
[2] J. Zimmerberg, S.S. Vogel, L.V. Chernomordik, Annu. Rev. Biophys. Biomol. Struct. 22 (1993) 433–466.
[3] S.R. Durell, I. Martin, J. Ruysschaert, Y. Shai, R. Blumenthal, Mol. Membr. Biol. 14 (1997) 97–112.
[4] W.R. Gallaher, Cell 50 (1987) 327–328.
[5] M.L. Bosch, P.L. Earl, K. Fargnoli, S. Picciafuoco, F. Giombini, F. Wong-Staal, G. Franchini, Science 244 (1989) 694–697.
[6] E.O. Freed, D.J. Myers, R. Risser, Proc. Natl. Acad. Sci. USA 87 (1990) 4650–4654.
[7] E.O. Freed, E.L. Delwart, G.L. Buchschacher, A.T. Panganiban, Proc. Natl. Acad. Sci. USA 89 (1992) 70–74.
[8] R.M. Epand, Biochim. Biophys. Acta 1376 (1998) 353–368.
[9] M. Rafalski, J. Lear, W. DeGrado, Biochemistry 29 (1990) 7917–7922.
[10] V.A. Slepushkin, S. Andreev, M. Sidorova, G.B. Melikyan, V.B. Grigoriev, V.M. Chumakov, A. Grinfeldt, R.A. Manukyan, E.V. Karamov, AIDS Res. Hum. Retroviruses 8 (1992) 9–18.
[11] L.M. Gordon, C. Curtain, Y.C. Zhong, A. Kirkpatrick, P. Mobley, A.J. Waring, Biochim. Biophys. Acta 1139 (1992) 257–274.
[12] I. Martin, F. Defrise-Quertain, E. Decroly, M. Vandenbranden, R. Brasseur, J. Ruysschaert, Biochim. Biophys. Acta 1145 (1993) 124–133.
[13] J.L. Nieva, S. Nir, A. Muga, F.M. Goñi, J. Wilschut, Biochemistry 33 (1994) 3201–3209.
[14] Y. Kliger, A. Aharon, D. Rapaport, P. Jones, R. Blumenthal, Y. Shai, J. Biol. Chem. 272 (1997) 13496–13505.
[15] I. Martin, H. Schaal, A. Scheid, J. Ruysschaert, J. Virol. 70 (1996) 298–304.
[16] D. Chang, S. Cheng, W. Chien, J. Virol. 71 (1997) 6593–6602.
[17] J.L. Nieva, S. Nir, J. Wilschut, J. Liposome Res. 8 (1998) 165–182.
[18] F.B. Pereira, F.M. Goñi, A. Muga, J.L. Nieva, Biophys. J. 73 (1997) 1977–1986.
[19] P.W. Mobley, A.J. Waring, M.A. Sherman, L.M. Gordon, Biochim. Biophys. Acta 1418 (1999) 1–18.
[20] M. Pritsker, P. Jones, R. Blumenthal, Y. Shai, Proc. Natl. Acad. Sci. USA 95 (1998) 7287–7292.
[21] M. Pritsker, J. Rucker, T.L. Hoffman, R.W. Doms, Y. Shai, Biochemistry 38 (1999) 11359–11371.
[22] G. Schwarz, S.E. Taylor, Biophys. J. 76 (1999) 3167–3175.
[23] F.B. Pereira, J.M. Valpuesta, G. Basañez, F.M. Goñi, J.L. Nieva, Chem. Phys. Lipids 103 (1999) 11–20.
[24] D.P. Siegel, J.L. Burns, Y. Talmon, Biophys. J. 56 (1989) 161–169.
[25] D.P. Siegel, W.J. Green, Y. Talmon, Biophys. J. 66 (1994) 402–414.
[26] P.M. Frederik, K.N.J. Burger, M.C.A. Stuart, A.J. Verkleij, Biochim. Biophys. Acta 1062 (1991) 133–141.
[27] G. Basañez, B. Ruiz-Argüello, A. Alonso, F.M. Goñi, G. Karlsson, K. Edwards, Biophys. J. 72 (1997) 2630–2637.
[28] D.P. Siegel, R.M. Epand, Biophys. J. 73 (1997) 3089–3111.
[29] B.L.S. Mui, P.R. Cullis, E.A. Evans, T.D. Madden, Biophys. J. 64 (1993) 443–453.
[30] B.L.S. Mui, H.G. Döbereiner, T.D. Madden, P.R. Cullis, Biophys. J. 69 (1995) 930–941.
[31] M.J. Hope, M.B. Bally, G. Webb, P.R. Cullis, Biochim. Biophys. Acta 812 (1985) 55–65.
[32] C.S.F. Böttcher, C.M. van Gent, C. Fries, Anal. Chim. Acta 24 (1961) 203–204.
[33] D.K. Struck, D. Hoekstra, R.E. Pagano, Biochemistry 20 (1981) 4093–4099.
[34] F.B. Pereira, F.M. Goñi, J.L. Nieva, FEBS Lett. 362 (1995) 243–246.
[35] C.R. Flach, A. Gericke, R. Mendelsohn, J. Phys. Chem. B 101 (1997) 58–65.
[36] E.J. Bolen, P.W. Holloway, Biochemistry 29 (1990) 9638–9643.

[37] A.I.P.M. De Kroon, M.W. Soekarjo, J. De Gier, B. De Kruijff, Biochemistry 29 (1990) 8229–8240.
[38] F. Moro, F.M. Goñi, M.A. Urbaneja, FEBS Lett. 330 (1993) 129–132.
[39] A. Gericke, E.R. Smith, D.J. Moore, R. Mendelsohn, J. Storch, Biochemistry 36 (1997) 8311–8317.
[40] D. Dieudonne, A. Gericke, C.R. Flach, X. Jiang, R.S. Farid, R. Mendelshon, J. Am. Chem. Soc. 120 (1998) 792–799.
[41] H. Mach, C. Russell Middaugh, Biochemistry 34 (1995) 9913–9920.
[42] T.J. McIntosh, P.W. Holloway, Biochemistry 26 (1987) 1783–1788.
[43] J. Brunner, FEBS Lett. 257 (1989) 369–372.
[44] M.L. Longo, A.J. Waring, D.A. Hammer, Biophys. J. 73 (1997) 1430–1439.
[45] K. Matsuzaki, O. Murase, H. Tokuda, S. Funakoshi, N. Fujii, K. Miyajima, Biochemistry 33 (1994) 3342–3349.
[46] B. Bechinger, J. Membr. Biol. 156 (1997) 197–211.
[47] A. Soloaga, M.P. Veiga, L.M. García-Segura, H. Ostolaza, R. Brasseur, F.M. Goñi, Mol. Microbiol. 31 (1999) 1013–1024.
[48] L.V. Chernomordik, V.A. Frolov, E. Leikina, P. Bronk, J. Zimmerberg, J. Cell Biol. 140 (1998) 1369–1382.
[49] W. Weissenhorn, A. Dessen, S.C. Harrison, J.J. Skehel, D.C. Wiley, Nature 387 (1997) 426–428.
[50] D. Chan, P.S. Kim, Cell 93 (1998) 681–684.
[51] L.V. Chernomordik, J. Zimmerberg, Curr. Opin. Struct. Biol. 5 (1995) 541–547.
[52] D.P. Siegel, Biophys. J. 76 (1999) 291–313.
[53] M.M. Kozlov, L.V. Chernomordik, Biophys. J. 75 (1998) 1384–1396.